Parasitic source resistance at different temperatures for AlGaN/AlN/GaN heterostructure field-effect transistors*

Yan Liu(刘艳)[1], Zhao-Jun Lin(林兆军)[1,†], Yuan-Jie Lv(吕元杰)[2], Peng Cui(崔鹏)[1], Chen Fu(付晨)[1], Ruilong Han(韩瑞龙)[1], Yu Huo(霍宇)[1], and Ming Yang(杨铭)[1]

[1] *School of Microelectronics, Shandong University, Jinan* 250100, *China*
[2] *National Key Laboratory of Application Specific Integrated Circuit (ASIC), Hebei Semiconductor Research Institute, Shijiazhuang* 050051, *China*

(Received 14 January 2017; revised manuscript received 23 April 2017; published online 31 July 2017)

The parasitic source resistance (R_S) of AlGaN/AlN/GaN heterostructure field-effect transistors (HFETs) is studied in the temperature range 300–500 K. By using the measured R_S and both capacitance–voltage (C–V) and current–voltage (I–V) characteristics for the fabricated device at 300, 350, 400, 450, and 500 K, it is found that the polarization Coulomb field (PCF) scattering exhibits a significant impact on R_S at the above-mentioned different temperatures. Furthermore, in the AlGaN/AlN/GaN HFETs, the interaction between the additional positive polarization charges underneath the gate contact and the additional negative polarization charges near the source Ohmic contact, which is related to the PCF scattering, is verified during the variable-temperature study of R_S.

Keywords: AlGaN/AlN/GaN heterostructure field-effect transistors (HFETs), parasitic source resistance, polarization Coulomb field scattering

PACS: 71.55.Eq, 73.40.Cg, 51.50.+v **DOI:** 10.1088/1674-1056/26/9/097104

1. Introduction

GaN-based heterostructure field-effect transistors (HFETs) are considered to be suitable for high temperature, high frequency, and high power applications. In GaN-based HFETs, the parasitic source resistance (R_S) is an important parameter for the device performance.[1,2] Here, R_S includes the gate-to-source access resistance (R_{GS}) and the Ohmic contact resistance (R_{Ohmic}), and it leads to some undesirable effects. For example, R_S reduces the effective transconductance of the device and the current gain cutoff frequency. It is necessary to analyze the origin and properties of R_S at different temperatures for enhancing the device performance in various environments. As previously known, R_S is related to the scattering mechanisms for the electrons in the gate–source channel. Both theoretical and experimental results reveal that the polarization Coulomb field (PCF) scattering is an important scattering mechanism in AlGaN/AlN/GaN HFETs.[3–5] Recently, the effect of the PCF scattering on R_S was verified at room temperature.[6] However, the influence of PCF scattering on R_S is unknown at elevated temperatures. Therefore, for the AlGaN/AlN/GaN HFETs, it is important to study the relationship between PCF scattering and R_S at elevated temperatures. In this study, we investigate the influence of PCF scattering on R_S in AlGaN/AlN/GaN HFETs in the temperature range 300–500 K using the measured temperature-dependent R_S and both capacitance–voltage (C–V) and current–voltage (I–V) characteristics of the prepared device.

2. Experiments

The undoped $Al_{0.28}Ga_{0.72}N$/AlN/GaN heterostructure layers used in this study were grown on a (0001) sapphire substrate by molecular beam epitaxy (MBE). Moreover, the components of its active structure were exhibited in detail in Fig. 1. The $Al_{0.28}Ga_{0.72}N$/AlN/GaN HFET was manufactured according to the standard process.[7] Its source and drain Ohmic metal stack comprised Ti/Al/Ni/Au. The source and drain regions were rectangular with a length and width of 50 μm and 100 μm, respectively. The drain-to-source distance was 100 μm. Ni/Au was deposited to form the gate Schottky contact. The size of the gate Schottky contact was 20 μm/100 μm (length/width), and the gate was 20 μm away from the source. The respective C–V measurements for the

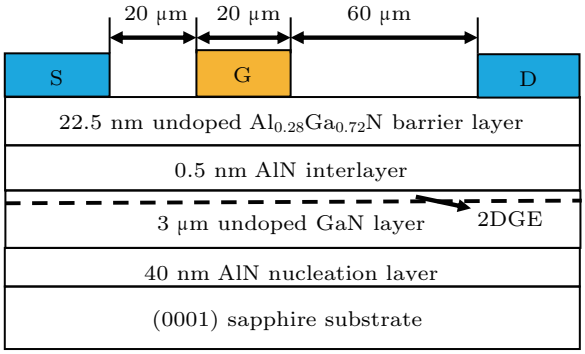


Fig. 1. (color online) Schematic cross section of fabricated AlGaN/AlN/GaN HFET.

*Project supported by the National Natural Science Foundation of China (Grant Nos. 11174182, 11574182, and 61306113) and the Specialized Research Fund for the Doctoral Program of Higher Education of China (Grant No. 20110131110005).

†Corresponding author. E-mail: linzj@sdu.edu.cn

© 2017 Chinese Physical Society and IOP Publishing Ltd

prepared $Al_{0.28}Ga_{0.72}N$/AlN/GaN HFET at 300, 350, 400, 450, and 500 K were performed using Agilent B1520A at 1 MHz. Moreover, the respective *I*–*V* and R_S measurements at the above different temperatures were performed using the Agilent B1500A semiconductor parameter analyzer.

3. Results and discussion

Figure 2(a) shows the measured *C*–*V* curves of the prepared $Al_{0.28}Ga_{0.72}N$/AlN/GaN HFET at different temperatures. The two-dimensional electron gas (2DEG) electron density (n_{2D}) can be obtained by the *C*–*V* curve integration, and the values are shown in Fig. 2(b).[8] Table 1 lists the values of n_{2D} corresponding to zero gate bias (n_{2D0}) at each testing temperature. Figure 3 displays the output characteristics at different temperatures for the prepared sample. The drain-current, I_{DS}, with a source–drain voltage of 125 mV at zero gate bias can be obtained from the *I*–*V* characteristics, and the values at different temperatures are shown in Table 1.

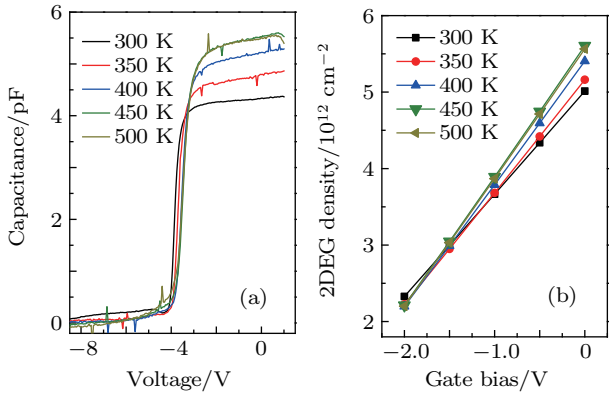


Fig. 2. (color online) (a) Measured *C*–*V* curves for $Al_{0.28}Ga_{0.72}N$/AlN/GaN HFET at different temperatures. (b) Obtained 2DEG electron sheet density n_{2D} from *C*–*V* measurements for the sample at different temperatures.

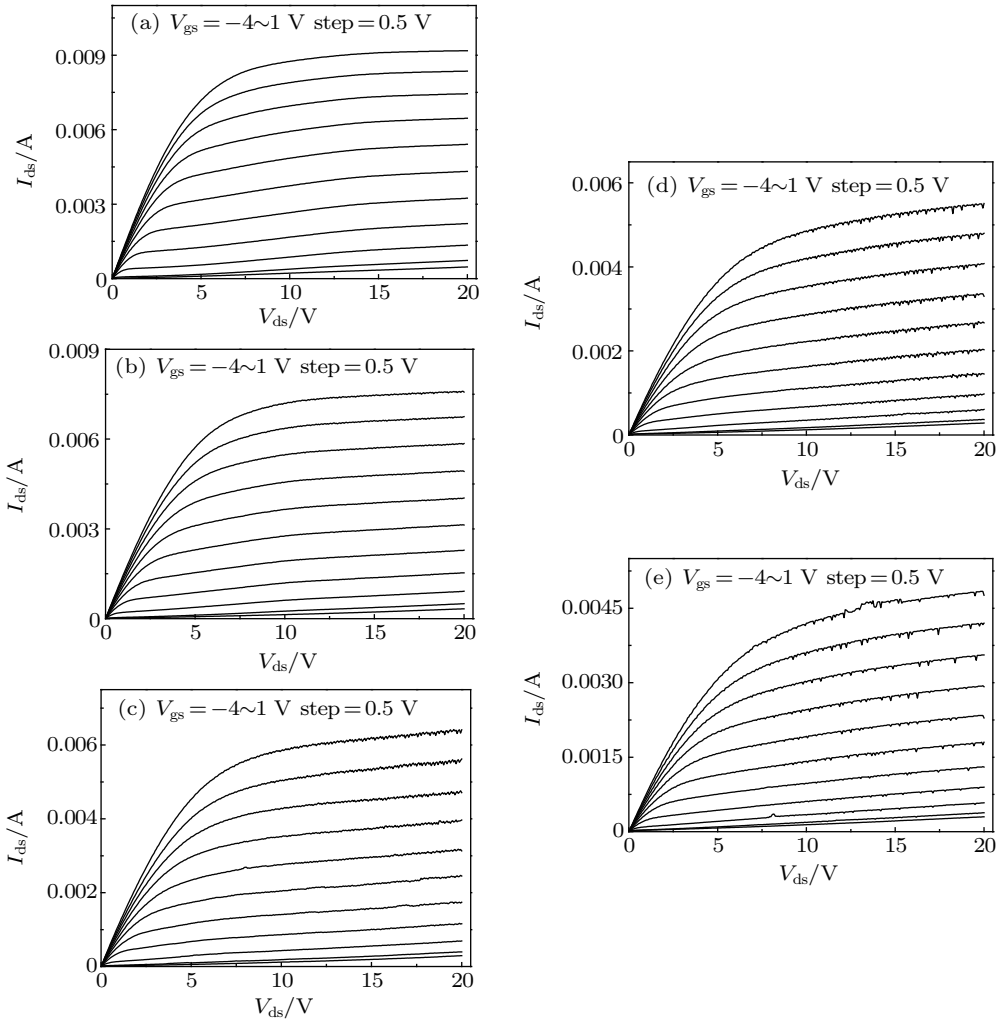


Fig. 3. Measured output characteristics of the sample at (a) 300 K, (b) 350 K, (c) 400 K, (d) 450 K, and (e) 500 K.

The 2DEG electron mobility corresponding to zero gate bias (μ_{n0}) at 300, 350, 400, 450, and 500 K for the prepared $Al_{0.28}Ga_{0.72}N$/AlN/GaN HFET can be obtained using the same method,[4] and the calculated results are shown in Table 1. Moreover, according to Ref. [4], the gate-to-source access resistance corresponding to zero gate bias (R_{GS0}) can

be calculated by

$$R_{GS0} = \frac{L_{GS}}{en_{2D0}\mu_{n0}W}, \quad (1)$$

where L_{GS} is the gate-to-source length, e is the electron charge, n_{2D0} and μ_{n0} are defined earlier, and W is the gate width. Here, it is noted that the Ohmic contact resistance, R_{Ohmic}, is not included in the calculated R_{GS0}. Using the transfer-length method (TLM),[9] the specific resistivity of the Ohmic contact is estimated to be 7.98×10^{-5} Ω·cm^2 at 300 K, and the value of R_{Ohmic} is calculated to be 26.09 Ω. Therefore, R_{S0} (R_{S0} is defined as the parasitic source resistance corresponding to zero gate bias), which is the sum of R_{GS0} and R_{Ohmic}, can be obtained. In addition, it is suggested that the Ohmic contact resistance for the AlGaN/GaN heterojunction exhibits a weaker dependence on temperature.[10] Moreover, in this study, the values of R_{Ohmic} at different temperatures can be obtained using the TLM, as shown in Fig. 4. Thus, R_{S0} at different temperatures can be determined, and the results are shown in Table 1.

Table 1. Parameters of the prepared AlGaN/AlN/GaN HFET at different temperatures. V_{GS} is the gate–source bias, V_{DS} is the drain–source bias, I_{DS} is the channel current, n_{2D0} is the 2DEG electron density at zero gate bias, μ_{n0} is the 2DEG electron mobility with zero gate bias, and R_{S0} is the parasitic source resistance corresponding to zero gate bias, which is the sum of the source access resistance and the Ohmic contact resistance.

T/K	V_{GS}/V	V_{DS}/mV	I_{DS}/mA	$n_{2D0}/10^{12}$ cm^{-2}	μ_{n0}/cm^2·V^{-1}·s^{-1}	R_{S0}/Ω
300	0	125	0.23465	5.01	2340.44	132.63
350	0	125	0.17338	5.16	1679.6	173.4
400	0	125	0.1325	5.41	1225.71	219.4
450	0	125	0.10818	5.61	964.94	260.07
500	0	125	0.087138	5.56	783.01	315.65

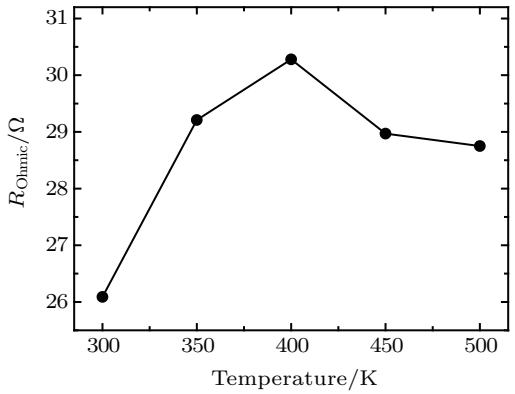


Fig. 4. Plot of R_{Ohmic} versus T for the sample.

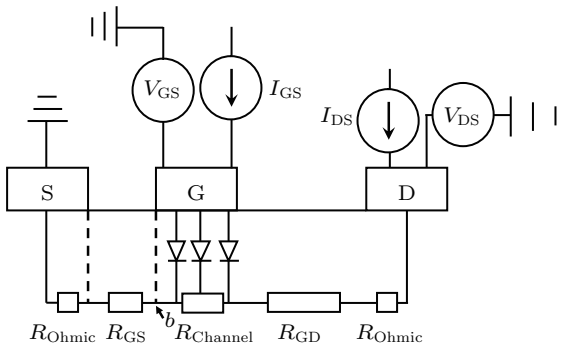


Fig. 5. Test configuration for measuring R_S using gate probe, I_{GS} = constant.

R_S can be measured using the gate probe method, as described in detail in Ref. [11]. The gate probe method shows that an accurate R_S can be extracted from the plot of the gate–source bias (V_{GS}) versus I_{DS} under the conditions of $I_{GS} \ll I_{DS}$, the relatively low drain-to-source bias (V_{DS}), and the constant forward gate–source current I_{GS}. Figure 5 is the test configuration for measuring R_S using the gate probe. As shown in Fig. 5, the gate was forward driven with a constant current I_{GS} and the drain was driven with a range of currents, while the source was grounded. As I_{GS} is fixed, the voltage drop across the gate Schottky barrier V_{drop} is constant. Therefore, V_{GS} is the sum of the channel voltage at the source edge of the gate (V_b) and V_{drop}. Owing to $V_b = I_{DS} \times (R_{Ohmic} + R_{GS})$, V_b increases with the increase of I_{DS} when V_{DS} increases. Here, R_{GS} is the gate-to-source access resistance. As $V_{GS} = V_b + V_{drop} = I_{DS} \times (R_{Ohmic} + R_{GS}) + V_{drop}$, the derivative of V_{GS} with respect to I_{DS} is the value of $R_{Ohmic} + R_{GS}$, that is, R_S.[1,6,11]

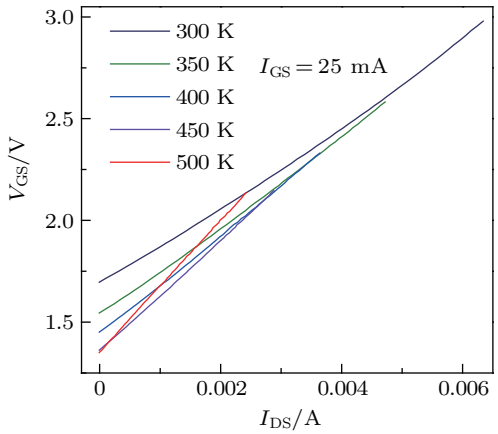


Fig. 6. (color online) Plot of V_{GS} versus I_{DS} at different temperatures with I_{GS} = 25 μA for the sample.

According to the gate probe method, the value of R_S is equal to the slope in the V_{GS} versus I_{DS} plot, and the prominent linear relationship of V_{GS} versus I_{DS} suggests that an accurate extraction of R_S can be obtained. In order to study the

effect of PCF scattering on R_S in the temperature range 300–500 K, the measurements of R_S were conducted at the same value of I_{GS} under the above different temperatures. Figure 6 shows the measured curves, that is, the plot of V_{GS} versus I_{DS} at different temperatures with forward gate current of 25 μA ($I_{GS} = 25$ μA). Here, the drain-to-source bias is maintained in the range from 0 V to 3 V. From Fig. 6, the value of R_S corresponding to $I_{GS} = 25$ μA at each testing temperature, R_{S25}, can be extracted. The black trace in Fig. 7 corresponds to the extracted R_{S25}. Moreover, the red trace in Fig. 7 corresponds to R_{S0} (the value of R_{S0} at each testing temperature is also listed in Table 1).

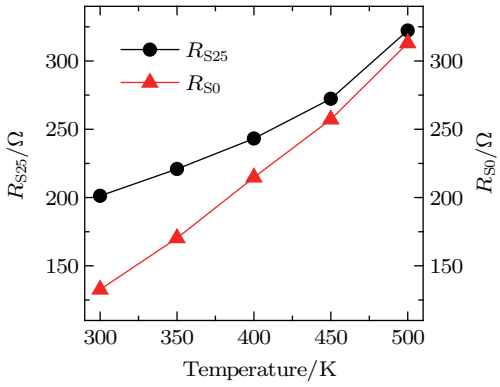


Fig. 7. (color online) Variations of R_{S25} (black trace) and R_{S0} (red trace) with temperature. R_{S25} represents the value of R_S at $I_{GS} = 25$ μA, and R_{S0} represents the value of R_S at $V_{GS} = 0$ V.

As observed from Fig. 7, R_{S25} is larger than R_{S0} at each corresponding testing temperature, and the resistance difference between R_{S25} and R_{S0} ($\Delta R_S = R_{S25} - R_{S0}$) decreases with increasing temperature. R_S is related to the scattering mechanisms and n_{2D} for the electrons in the gate–source channel. As n_{2D} in the gate–source channel is not modulated by the gate–source bias V_{GS},[4] the value of n_{2D} in the gate–source channel is assumed to remain unchanged as V_{GS} or I_{GS} varies. It indicates that the value of n_{2D} in the gate–source channel corresponding to $I_{GS} = 25$ μA is equal to that corresponding to $I_{GS} = 0$ μA at the same temperature. Therefore, R_{S25} and R_{S0} correspond to the same value of n_{2D} at the same temperature. Hence, the resistance difference, ΔR_S, does not result from n_{2D} of the gate–source channel.

In undoped AlGaN/AlN/GaN HFETs, the longitudinal optical (LO) phonon scattering, the interface roughness (IFR) scattering, and the PCF scattering are primarily the three types of important scattering mechanisms.[3,4] For LO phonon scattering, it is primarily related to the average phonon number and n_{2D}. For IFR scattering, it is mostly determined by the average distance of the 2DEG electrons from the AlN/GaN interface. The average phonon number is primarily determined by temperature, and the average distance of the 2DEG electrons from the AlN/GaN interface is considerably impacted by n_{2D}. As mentioned earlier, n_{2D} in the gate–source channel does not vary with I_{GS}. Therefore, for both LO phonon and IFR scatterings, they are I_{GS}-independent at the same temperature. Hence, both LO phonon and IFR scatterings cannot lead to the difference between R_{S25} and R_{S0} at the same temperature.

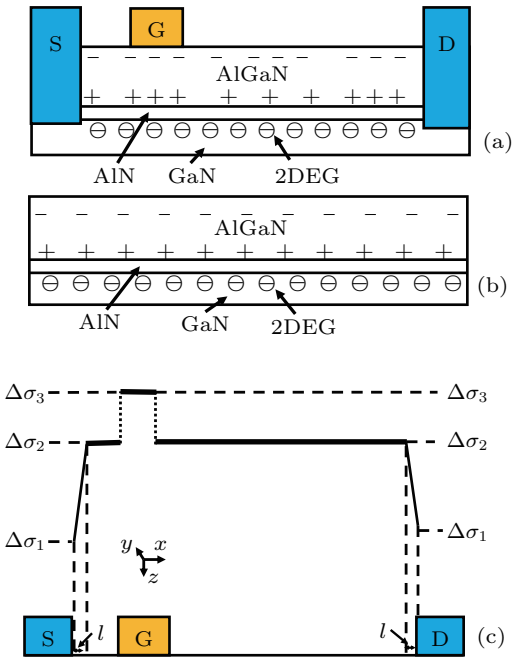


Fig. 8. (color online) Schematic of polarization charges distribution. (a) Distribution of polarization charges with the Ohmic and Schottky contact metals. (b) Distribution of polarization charges without the contact metals. (c) Distribution of the additional polarization charge density. +: Positive polarization charges; —: Negative polarization charges; ⊖: Two-dimensional electron gas electrons.

For PCF scattering as one of the primary types of important scattering mechanisms in AlGaN/AlN/GaN HFETs as mentioned earlier, it is closely related to the distribution of the polarization charges along the AlGaN/AlN/GaN heterostructure interface. The detailed illustration is provided in the following. The distribution of the polarization charges at the AlGaN/AlN/GaN heterostructure interface using the device processing mechanism and both the gate–source and drain–source biases is not uniform (see Fig. 8(a)). Without the deposition of the contact metals, the distribution of the polarization charges at the AlGaN/AlN/GaN heterostructure material interface is uniform (see Fig. 8(b)). The difference between the nonuniform polarization (Fig. 8(a)) and the uniform polarization (Fig. 8(b)) is considered as the additional polarization charges. Figure 8(c) provides the distribution of the additional polarization charge density. In Fig. 8(c), $\Delta\sigma_1$ is the additional negative polarization charge density near the Ohmic contact metals, which is generated by the Ohmic-contact processing owing to the diffusion of the Ohmic contact metal atoms. l is the diffusion length of the Ohmic contact metal atoms.[4] $\Delta\sigma_1$ and l are related to the Ohmic contact processing only and not modulated by the gate bias and temperature. $\Delta\sigma_2$ is the additional polarization charge density under the ungated region

except the range of l. Neither the Ohmic-contact processing nor the bias voltage influence $\Delta\sigma_2$. Hence, the value of $\Delta\sigma_2$ is considered to be 0.[3,4] $\Delta\sigma_3$ is the positive additional polarization charge density underneath the gate, which is induced by the forward gate–source bias owing to the converse piezoelectric effect.

The PCF scattering theory indicates that the additional polarization charges establish the elastic scattering potential that scatters 2DEG electrons, and the larger the PCF scattering potential is, the stronger the PCF scattering will be.[3–5] Here, the PCF scattering potential, $V(x,y,z)$, can be expressed as[6]

$$\begin{aligned} V(x,y,z) = & -\frac{e}{4\pi\varepsilon_s\varepsilon_0}\int_{-L_{GS}-\frac{L_G}{2}}^{-L_{GS}-\frac{L_G}{2}+l} \mathrm{d}x' \\ & \times \int_0^W \frac{\Delta\sigma_1(-x'-L_G/2-L_{GS}+l)}{l\sqrt{(x-x')^2+(y-y')^2+z^2}}\mathrm{d}y' \\ & -\frac{e}{4\pi\varepsilon_s\varepsilon_0}\int_{-\frac{L_G}{2}}^{\frac{L_G}{2}} \mathrm{d}x' \\ & \times \int_0^W \frac{\Delta\sigma_3}{\sqrt{(x-x')^2+(y-y')^2+z^2}}\mathrm{d}y' \\ & -\frac{e}{4\pi\varepsilon_s\varepsilon_0}\int_{\frac{L_G}{2}+L_{GD}-l}^{\frac{L_G}{2}+L_{GD}} \mathrm{d}x' \\ & \times \int_0^W \frac{\Delta\sigma_1(x'-L_G/2-L_{GD}+l)}{l\sqrt{(x-x')^2+(y-y')^2+z^2}}\mathrm{d}y'. \end{aligned} \quad (2)$$

From Eq. (2), it can be observed that the magnitude of the PCF scattering potential relates to the diffusion length of the Ohmic contact metal atoms l, the additional polarization charge density $\Delta\sigma_1$ and $\Delta\sigma_3$, and the device structure parameters such as the gate–source length L_{GS}, the gate length L_G, the gate–drain length L_{GD}, and the device width W. For the same device studied in this paper, the device structure parameters are the same and do not vary with the gate bias and temperature. In addition, as mentioned earlier, as $\Delta\sigma_1$ and l are related to the Ohmic contact processing only, the values of $\Delta\sigma_1$ and l for the sample remain constant at different gate biases and temperatures. For R_{S25} and R_{S0} in Fig. 7, they correspond to $I_{GS} = 25$ μA and $I_{GS} = 0$ μA, respectively. At the same temperature, the voltage drop across the gate Schottky barrier, V_{drop}, corresponding to $I_{GS} = 25$ μA, is higher than that corresponding to $I_{GS} = 0$ μA ($V_{GS} = 0$ V). Thus, owing to the converse piezoelectric effect, the value of $\Delta\sigma_3$ corresponding to $I_{GS} = 25$ μA is larger than that corresponding to $I_{GS} = 0$ μA at the same temperature, which results in a magnitude of the PCF scattering potential corresponding to $I_{GS} = 25$ μA that is larger than that corresponding to $I_{GS} = 0$ μA. As a result, the PCF scattering corresponding to $I_{GS} = 25$ μA is stronger than that corresponding to $I_{GS} = 0$ μA at the same temperature. Therefore, the resistance difference between R_{S25} and R_{S0}, ΔR_S, results from PCF scattering. Moreover, R_{S25} is larger than R_{S0} at the same temperature, as shown in Fig. 7.

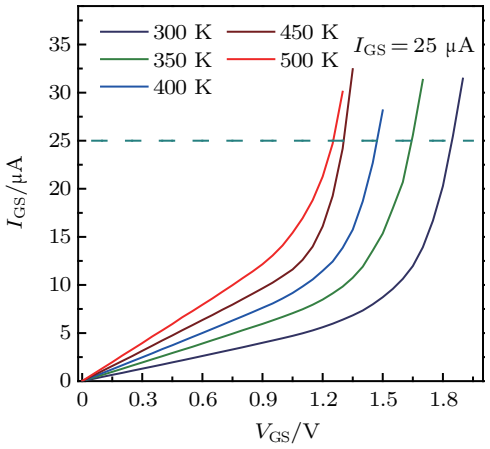


Fig. 9. (color online) Measured forward I–V characteristics of Ni/Au/AlGaN/AlN/GaN Schottky diode at different temperatures.

The polarization charges along the AlGaN/AlN/GaN interface involve both spontaneous and piezoelectric polarization. The spontaneous polarization does not vary with gate bias,[4] and seldom changes with temperature.[12,13] Hence, the variation of ΔR_S with temperature is closely related to the AlGaN barrier layer piezoelectric polarization. The piezoelectric polarization varies with z-direction electric field in the AlGaN barrier layer owing to the converse piezoelectric effect, and it is expressed as[14]

$$P_{PE,AlGaN} = E_{PE,AlGaN}\frac{e_{33}^2}{C_{33}}, \quad (3)$$

where $P_{PE,AlGaN}$ is the piezoelectric polarization charge density, C_{33} is the elastic constant of AlGaN, e_{33} is piezoelectric constant, $E_{PE,AlGaN} = V_{drop}/d_{AlGaN}$ is the biased z-direction electric field in the AlGaN barrier layer, and d_{AlGaN} is the AlGaN barrier layer thickness. As the voltage drops across both the gate–source channel and the Ohmic contact, that is, $I_{GS} \times (R_{Ohmic} + R_{GS})$ are negligible compared to the voltage drop across the gate Schottky barrier V_{drop} for all the testing temperatures when I_{GS} is equal to 25 μA, it is reasonable to assume that V_{drop} is approximately equal to V_{GS}. V_{GS} at different temperatures corresponding to $I_{GS} = 25$ μA can be obtained from Fig. 9, which provides the forward I–V characteristics of the gate–source Schottky diode at different temperatures.[6] Thus, the biased z-direction electric field $E_{PE,AlGaN}$ at different temperatures corresponding to $I_{GS} = 25$ μA can be determined. According to Eq. (3), the piezoelectric polarization charge density at different temperatures corresponding to $E_{PE,AlGaN}$ can also be obtained. Here, as C_{33} and e_{33} are considered temperature-independent,[15–18] the values of C_{33} and e_{33} for $Al_{0.28}Ga_{0.72}N$ barrier layer can be used as 396 GP and 0.93 C/m^2, respectively, in the above calculation.[19] Figure 10 provides these calculated results at different temperatures corresponding to $I_{GS} = 25$ μA, the black trace and the red trace

correspond to $E_{PE,AlGaN}$ and $P_{PE,AlGaN}$, respectively. As shown in Fig. 10, both the piezoelectric polarizations corresponding to $I_{GS} = 25$ μA and the biased z-direction electric field decrease with increasing temperature. The piezoelectric polarization charge density in Eq. (3) is precisely the additional positive polarization charge density underneath the gate, that is, $\Delta\sigma_3$ in Fig. 8(c), which is proportional to the PCF scattering intensity. Therefore, the PCF scattering decreases for the prepared AlGaN/AlN/GaN HFET with increasing temperature. Thus, the resistance difference, ΔR_S, decreases with increasing temperature, as shown in Fig. 7.

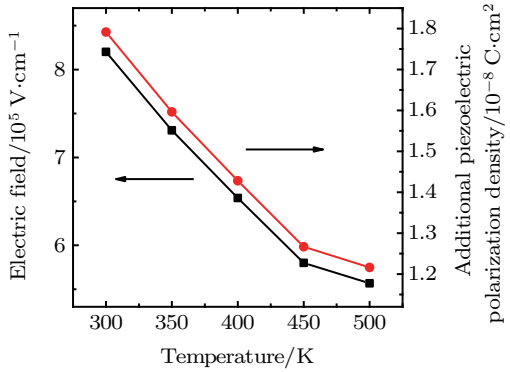


Fig. 10. (color online) Variations of electric field and piezoelectric polarization of AlGaN barrier layer corresponding to $I_{GS} = 25$ μA at different temperatures.

In addition, figure 10 shows that the biased z-direction electric field ($E_{PE,AlGaN} = 5.57 \times 10^5$ V/cm) at 500 K is still strong. Figure 7 shows the resistance difference ΔR_S at 500 K is considerably small. The reason can be explained below.

As mentioned earlier, the Ohmic-contact processing can generate the additional negative polarization charge density near the Ohmic contact metals, that is, $\Delta\sigma_1$ in Fig. 8(c). The positive gate–source bias corresponding to the forward gate current of 25 μA can generate the piezoelectric polarization charge density under the gate, that is, the additional positive polarization charge density underneath the gate contact, that is, $\Delta\sigma_3$ in Fig. 8(c). The scattering potential of the PCF scattering corresponding to $I_{GS} = 0$ μA ($V_{GS} = 0$ V) is only constituted by $\Delta\sigma_1$. The scattering potential of the PCF scattering corresponding to $I_{GS} = 25$ μA is constituted by $\Delta\sigma_1$ and $\Delta\sigma_3$. From Eq. (2), the PCF scattering potential between $\Delta\sigma_1$ and $\Delta\sigma_3$ can be eliminated. As mentioned earlier, as $\Delta\sigma_1$ do not vary with both temperature and gate bias, and $\Delta\sigma_3$, which is the piezoelectric polarization charge density induced by V_{drop}, decreases with increasing temperature. It can be inferred that the difference in the absolute value of $\Delta\sigma_1$ and $\Delta\sigma_3$ decreases with increasing temperature, and the absolute value of the above difference is approximately equal to that of $\Delta\sigma_1$ at 500 K. As a result, the scattering potential of PCF scattering corresponding to $I_{GS} = 25$ μA is approximately equal to that corresponding to $I_{GS} = 0$ μA ($V_{GS} = 0$ V). Therefore, R_{S25} and R_{S0} at 500 K are approximately equal. Thus, although the z-direction biased electric field $E_{PE,AlGaN}$ at 500 K is still strong, the resistance difference ΔR_S is considerably small. Hence, all the above analysis shows that the PCF scattering exhibits an important influence on the parasitic source resistance R_S in the temperature range 300–500 K. This indicates that PCF scattering should be considered at elevated temperatures. In addition, the interaction between the positive additional polarization charges underneath the gate contact and the negative additional polarization charges near the source contact, which is related to PCF scattering, was verified during the variable-temperature study of R_S in the temperature range 300–500 K. Moreover, the PCF scattering, as a type of Coulomb field scattering, is related to distance. The shorter the gate–source spacing of the AlGaN/AlN/GaN HFETs is, the closer is the distance between the additional polarization charges and the 2DEG in the gate–source channel, and the stronger is the PCF scattering at elevated temperatures. Further research should be performed for the dependence of R_S on temperature, which is based on PCF scattering being the dominant mechanism in the AlGaN/AlN/GaN HFETs with the shorter gate–source distance.

4. Conclusions

In this study, we analyzed and studied the influence of PCF scattering on the parasitic source resistance R_S using the measured C–V and I–V characteristics and R_S in the temperature range 300–500 K for the prepared $Al_{0.28}Ga_{0.72}N$/AlN/GaN HFET. The results indicate that the PCF scattering should be considered at elevated temperatures as it was found to exhibit an important influence on R_S in the investigated temperature range. In addition, the interaction between the positive additional polarization charges underneath the gate contact and the negative additional polarization charges near the source contact was verified to influence the intensity of the PCF scattering.

References

[1] Palacios T, Rajan S, Chakraborty A, Heikman S, Keller S, DenBaars S P and Mishra U K 2005 *IEEE Trans. Electron Devices* **52** 2117
[2] Cao Z F, Lin Z J, Lv Y J, Luan C B, Yu Y X, Chen H and Wang Z G 2012 *Chin. Phys. B* **21** 017103
[3] Zhao J Z, Lin Z J, T D Corrigan, Wang Z, You Z D and Wang Z G 2007 *Appl. Phys. Lett.* **91** 173507
[4] Luan C B, Lin Z J, Lv Y J, Zhao J T, Wang Y T, Chen H and Wang Z G 2014 *J. Appl. Phys.* **116** 044507
[5] Zhao J T, Lin Z J, Luan C B, Zhou Y, Yang M, Lv Y J and Feng Z H 2014 *Appl. Phys. Lett.* **105** 083501
[6] Yang M, Lin Z J, Zhao J T, Cui P, Fu C and Lv Y J 2016 *IEEE Trans. Electron Devices* **63** 1471
[7] Lv Y J, Feng Z H, Gu G D, Dun S B, Yin J Y, Han T T, Sheng B C, Cai S J, Liu B and Lin Z J 2013 *Chin. Phys. B* **22** 077102
[8] Lin Z J, Zhao J Z, Corrigan T D, Wang Z, You Z D, Wang Z G and Wu L 2008 *J Appl. Phys.* **103** 044503
[9] Cohen S S 1983 *Thin Solid Films* **104** 361

[10] Fontseré A, Pérez-Tomaás A, Plácidi M, Fernández-Martínez P, Baron N, Chenot S, Cordier Y, Moreno J C, Jennings M R, Gammon P M and Walker D 2011 *Proc. 8th Spanish Conf. Electron Devices* 1–2
[11] Holmstrom R P, Bloss W L and Chi J Y 1986 *IEEE Electron. Dev. Lett.* **EDL-7** 410
[12] Ambacher O, Majewski J, Miskys C, Link A, Hermann M, Eickhoff M, Stutzmann M, Bernardini F, Fiorentini V, Tilak V, Schaff B and Eastman L F 2002 *J. Phys. Condens. Matter* **14** 3399
[13] Bykhovski A D, Kaminski V V, Shur M S, Chen Q C and Khan M A 1996 *Appl. Phys. Lett.* **69** 3254
[14] Anwar A F M, Webster R T and Smith K V 2006 *Appl. Phys. Lett.* **88** 203510
[15] Reeber R R and Wang K 2001 *MRS Internet J. Nitride Semicond. Res.* **6** 1
[16] Deger C, Born E, Angerer H, Ambacher O, Stutzmann M, Hornsteiner J, Riha E and Fischerauer G 1998 *Appl. Phys. Lett.* **72** 2400
[17] Roder C, Einfeldt S, Figge S and Hommel D 2005 *Phys. Rev. B* **72** 085218
[18] Figge S, Kröncke H, Hommel D and Epelbaum B M 2009 *Appl. Phys. Lett.* **94** 101915
[19] Zhao J T, Lin Z J, Luan C B, Chen Q Y, Yang M, Zhou Y, Lv Y J and Feng Z H 2015 *Superlattices Microstruct.* **79** 21